Available online at www.sciencedirect.com
SCIENCE DIRECT®
Journal of Chromatography A, 995 (2003) 109–118
JOURNAL OF CHROMATOGRAPHY A
www.elsevier.com/locate/chroma

Identification of acylated xanthone glycosides by liquid chromatography–atmospheric pressure chemical ionization mass spectrometry in positive and negative modes from the lichen *Umbilicaria proboscidea*

Tomáš Řezanka[a,*], Valery M. Dembitsky[b]

[a]*Institute of Microbiology, Vídeňská 1083, Prague 14220, Czech Republic*
[b]*Department of Pharmaceutical Chemistry and Natural Products School of Pharmacy, P.O. Box 12065, Hebrew University of Jerusalem, Jerusalem 91120, Israel*

Received 24 December 2002; received in revised form 12 March 2003; accepted 14 March 2003

Abstract

The xanthoside composition of the crude extract of *Umbilicaria proboscidea* (L.) Schrader was characterized using LC–UV diode array detection and LC–atmospheric pressure chemical ionization (APCI) MS methods. The presence of acylated xanthone-*O*-glucosides was determined by both positive and negative ion LC–APCI-MS methods. Based on UV and MS spectral data and NMR spectroscopy, a total of 14 compounds (6-*O*-acylated umbilicaxanthosides A and B) were identified in *U. proboscidea* for the first time. In order to further develop the applicability of LC–MS techniques in phytochemical characterization, the effect of different ionization energy on fragmentation was studied using APCI. The optimal ionization conditions were achieved in positive ion APCI by using ammonium acetate buffer and in negative ion APCI by using formic acid (pH 4).

Keywords: *Umbilicaria proboscidea*; Plant materials; Xanthone glycosides, acylated; Glycosides

1. Introduction

The screening of crude plant extracts for the detection of prenylate xanthones is routinely performed by LC–UV [1]. The characterization of the analytes usually involves the separation and collection of each compound, followed by MS and NMR analyses [2–6]. Major drawbacks of such screening methods are the time and effort spent in identifying previously known compounds, as standards are usually unavailable from commercial sources. It has long been recognized that this problem can be solved, at least partially, by using directly combined LC–MS methods [2]. MS has the potential to yield structural information about the analytes in addition to their molecular mass. A major breakthrough in the application of LC–MS methods has come with the development and commercialization of various interfaces involving an atmospheric pressure chemical ionization (APCI) interface. Although APCI methods

*Corresponding author. Tel.: +420-2-4106-2300; fax: +420-2-4106-2347.
E-mail address: rezanka@biomed.cas.cz (T. Řezanka).

0021-9673/03/$ – see front matter
doi:10.1016/S0021-9673(03)00501-6

involve soft ionization techniques that produce mainly pseudomolecular ions, structural information can be obtained by the application of an electrostatic potential at the entrance to the quadrupole mass analyzer, which creates suitable conditions resulting in fragment ions.

This paper describes the use of LC–APCI-MS for the analysis of a crude methanol extract of the Central Asian lichen *Umbilicaria proboscidea* (L.) Schrader = Syn.: *Gyrophora proboscidea* (L.) Ach.

Fragmentation of the analyte molecules induced by application of variable voltage at the entrance to the quadrupole mass analyzer provided unique mass spectra for the majority of the compounds present in the sample. ^{1}H and ^{13}C NMR data were used to identify the position of acyl chain connected to the acylated xanthosides with similar fragmentation patterns present in the extract. Fragmentation pathways consistent with the observed data for acylated xanthosides are proposed.

2. Experimental

The specimen of the lichen *Umbilicaria proboscidea* was collected in August 2001 in Ural Mountains, Muslimovo Village, 50 km from Chelyabinsk (Russia). The voucher specimen is deposited in the collection of the second author (V.M. Dembitsky).

The aqueous–MeOH layer was obtained by the Blight and Dyer method [9] of lipid extraction from 100 g of air-dried lichen as previously described [7]. The extract was separated on a Sephadex LH-20 column; elution with MeOH gave two fractions of yellow oil, which were further separate chromatographed by an LC–APCI-MS system.

The instrument used for analysis of acylated xanthosides was a Hewlett-Packard model 1100 liquid chromatograph–mass-selective detector with an independent acquisition of both ultraviolet (diode array detector, 220–500 nm) and mass spectral data (mass selective detector). HP 1100 consists of the following components: autosampler, diaphragm solvent degasser, binary pump, diode array UV–VIS detection (DAD) system and the LC–MS system. Two Hichrom HIRPB-250AM 250×2.1 mm I.D., 5-μm phase particle columns were connected in series to obtain a high efficiency column of approximately ~53 000 plates/50 cm. The samples were separated using a gradient solvent program with different pH modifiers: initial from water–CH_3CN–CH_2Cl_2 (60:30:10, v/v/v); linear from 10 to 40 min to water–CH_3CN–CH_2Cl_2 (30:40:30, v/v/v); held until 60.5 min; the composition was returned to the initial conditions over 8 min. A peak threshold of 0.3% intensity was applied to the mass spectra. The eluent flow-rate was 0.6 ml/min, the column temperature was 28 °C, and the volume of injected sample was 20 μl. The following pH modifiers were used: 0.1% formic acid (pH 2.6), pH-adjusted formic acid (pH 4.0), 10 m*M* $AcONH_4$ at pH 5.0, 6.0 and 7.0 (pH adjusted with NH_4OH).

We operated the MS system in the positive or negative APCI mode. The parameters for the acquisition of mass spectral data were the following: scan range *m*/*z* 200–1200; capillary voltage setting, 1500 V; corona current, 10 μA; nebulizer pressure, 60 p.s.i. (1 p.s.i.=6894.76 Pa); drying gas flow, 4 l/min; drying gas temperature, 350 °C; vaporizer temperature, 500 °C; threshold, 150 counts; gain, 5; step size, 0.25 u; peak width, 0.1 min; fragmenter settings, 40 V and/or 140 V for positive and −30 V and/or −110 V for negative mode. Data acquisition and analyses were performed using Agilent ChemStation for LC–MS with ^{3D}LC ChemStation software.

Collection of material from several LC runs and removal of solvent by lyophilization yielded the major individual compound (**1a**). The lyophilized compound was dissolved in C^2HCl_3–$C^2H_3O^2H$ and the ^{1}H and ^{13}C NMR spectra were measured using a Bruker AMX 500 spectrometer (Bruker Analytik, Karlsruhe, Germany) at 500.1 MHz (^{1}H) and 125.7 MHz (^{13}C).

Mild hydrolysis with a base was performed as described in Ref. [7]. The fatty acid composition was determined by GC–MS after transmethylation with 5% HCl in methanol [7]. The sugar composition was also determined by GC–MS of trimethylsilyl derivatives after hydrolysis [7]. The aglycone composition was determined by MS and NMR spectra as previously described [7].

GC–MS of the fatty acid methyl esters and trimethylsilyl derivatives of saccharides was done using a Finnigan 1020 B single-state quadrupole

GC–MS instrument in the EI mode. The acids were methylated by heating them with 5% anhydrous HCl in MeOH, and the fatty acid methyl esters were further chromatographed using a fused-silica capillary column of chemically bonded liquid phase (Supelcowax 10, 60 m×0.2 mm I.D., Supelco) and helium carrier gas at a flow-rate of 0.35 ml min^{-1}. The column temperature was programmed from 50 °C held for 1 min, to 100 °C at a rate of 10 °C min^{-1}, and was then raised to the final hold temperature of 270 °C at a rate of 5 °C min^{-1}. The mass spectra of methyl esters agreed with previously published data [10].

The saccharides were dissolved in pyridine and BSA [*N*,*O*-bis(trimethylsilyl)acetamide] was added to this solution which was left to stand 30 min. The derivatives were then chromatographed under conditions described for above.

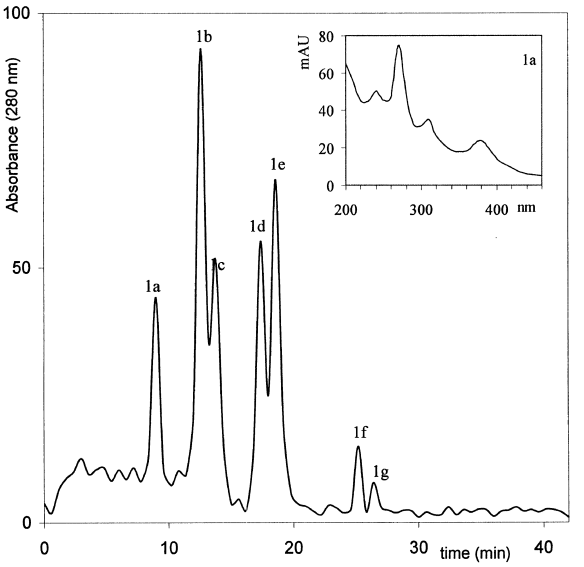

Fig. 1. The photodiode array UV chromatogram at 280 nm (**1a**–**1g**) with spectrum showing the characteristic absorption bands of linolenoyl umbilicaxanthosides B (**1a**) (**1a**, right upper corner).

3. Results and discussion

The methanol extract from the lichen was recently examined [7] and was found to contain two xanthosides, umbilicaxanthoside A and B, which have not yet been already reported. In addition, new acylated xanthosides are described in this paper.

The MeOH extract from the lichen *U. proboscidea* was subjected to gel filtration through Sephadex LH-20 to obtain two fractions (1 and 2). Table 1 gives the data obtained after LC from the two fractions. Fraction 1 (Fig. 1, acylated umbilicaxanthosides B) weighed 14.7 mg, fraction 2 (Fig. 2, acylated umbilicaxanthosides A) 2.3 mg. Fig. 1 shows the photodiode array UV chromatogram at 280 nm with a spectrum showing the characteristic absorption bands of linolenoyl umbilicaxanthosides B (Fig. 1a). The UV spectra (200–450 nm) were recorded on-line. All acylated xanthosides exhibited very similar, if not identical, UV spectra. Substitution by any acyl chain did not modify the chromophore [8]. All the above-mentioned data lead to the conclusion that the UV spectra of all 14 compounds are very similar and do not provide a clue for identification of the appropriate structures.

The components of acylated glucosides were also

Table 1
Composition in relative percent of acylated umbilicaxanthosides B (**1a**–**1g**) and A (**2a**–**2g**) from lichen of *U. proboscidea*

Compound	Acylated umbilicaxanthosides B (**1**)			Acylated umbilicaxanthosides A (**2**)		
	DAD	MS	GC–MS	DAD	MS	GC–MS
a (18:3)	13.2	12.7	12.8	12.5	10.9	10.8
b (18:2)	27.9	25.8	26.6	23.1	21.6	21.1
c (16:1)	15.4	15.2	16.2	9.9	9.9	9.8
d (18:1)	16.5	16.7	17.1	25.3	25.1	26.3
e (16:0)	20.2	21.4	20.0	18.2	20.0	19.8
f (20:1)	4.5	5.5	4.7	6.8	7.4	6.9
g (18:0)	2.3	2.7	2.6	4.2	5.1	5.3

From 100 g of air dried lichen was obtained 14.7 mg of total acylated umbilicaxanthosides B (fraction 1) and 2.3 mg of total acylated umbilicaxanthosides A (fraction 2).

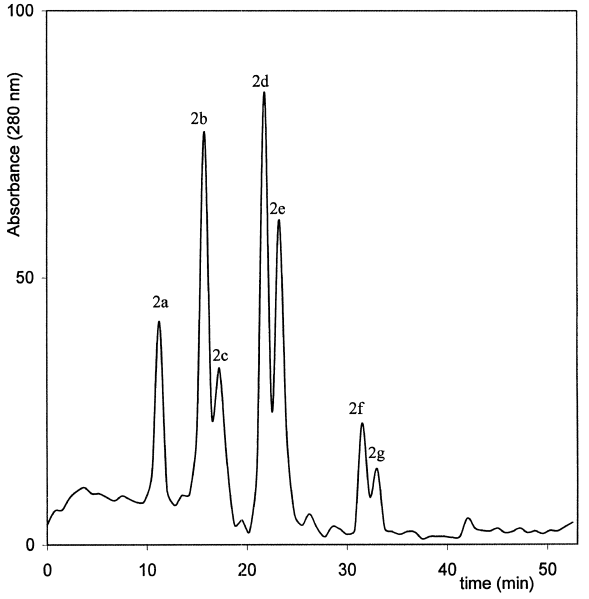

Fig. 2. The photodiode array UV chromatogram at 280 nm of umbilicaxanthosides A (**2a**–**2g**).

analyzed by GC after hydrolysis. Fractions 1 and 2 (after separation on Sephadex LH-20) contained umbilicaxanthones B and A as the aglycone moieties. Glucose was the only sugar detected in both homologous series. Furthermore, both series contained fatty acids. The fatty acid composition, which was identical with the results obtained from APCI analysis, was also determined by GC–MS (see Table 1).

Optimum APCI conditions were established by using samples of umbilicaxanthoside A and B previously purified from the crude extract [7]. The different fragmenter voltage settings used throughout this study and different cone voltage was shown to have a significant impact on their fragmentation patterns. The fragmentation of the xanthosides required two different voltage values (for positive and negative modes, respectively). If the cone voltage was set at 40 V in the positive mode, all compounds exhibited strong $[M+H]^+$ peaks but no fragmentation was observed. The following discussion of the APCI mass spectra of the acylated xanthosides studied here includes speculative assignments of fragmentation pathways for each compound analyzed (Tables 2–5).

The eluent compositions tested with APCI are presented in Experimental. The pH modifiers satisfied the volatility requirements, and covered the pH range within the stability limits of the silica-based bonded stationary phase. The use of different eluents produced the same elution order but much worse chromatographic resolutions.

The results of positive ion APCI show that the best sensitivity is achieved with eluents that contain only ammonium acetate at pH 5. The use of different pH leads to decrease of sensitivity. Further, with decreasing concentration of ammonium acetate the resolution of all acylated xanthosides is also dropping. The addition of acetate significantly changes the composition of the protonated gas phase of reactant ions. The decreased sensitivity may be due to non-formation of ions in positive ion APCI and their ability to neutralize positive charges.

Sensitivity was clearly increased by raising the temperature from 350 to 500 °C, especially for acylated glycosides. The increase in the probe temperature had no significant effect on the fragmenta-

Table 2
Positive APCI of **1a**–**1g**

	1a		**1b**		**1c**		**1d**		**1e**		**1f**		**1g**	
	18:3	%[a]	18:2	%	16:1	%	18:1	%	16:0	%	20:1	%	18:0	%
$[M+H]^+$	995	100	997	100	971	100	999	100	973	100	1027	100	1001	100
$[M+H-Glc]^+$	833	58	835	42	809	54	837	45	811	56	865	46	839	42
$[M+H-RCO]^+$	734	20	734	19	734	17	734	17	734	16	734	14	734	15
$[M+H-Glc-RCO]^+$	572	27	572	29	572	32	572	31	572	32	572	28	572	29
$[M+H-2\times Glc-RCO]^+$	410	66	410	74	410	64	410	80	410	86	410	62	410	73
$[M+H-2\times Glc-RCO-C_4H_8]^+$	354	14	354	15	354	14	354	14	354	13	354	14	354	13
$[M+H-2\times Glc-RCO-2\times C_4H_8]^+$	298	12	298	10	298	9	298	9	298	10	298	11	298	10

[a] Percent of base peak.

Table 3
Negative APCI of **1a**–**1g**

	1a		**1b**		**1c**		**1d**		**1e**		**1f**		**1g**	
	18:3	%[a]	18:2	%	16:1	%	18:1	%	16:0	%	20:1	%	18:0	%
$[M-H]^-$	993	88	995	85	969	76	997	79	971	67	1025	83	999	70
$[M-H-Glc]^-$	831	24	833	19	807	23	835	20	809	19	863	18	837	17
$[M-H-R_1C=C=O]^-$	733	21	733	17	733	19	733	16	733	17	733	14	733	14
$[M-H-RCOOH]^-$	715	65	715	54	715	61	715	48	715	57	715	54	715	48
$[M-H-2\times Glc-RCOOH]^-$	391	13	391	9	391	11	391	12	391	9	391	8	391	7
$[RCOO]^-$	277	100	279	100	253	100	281	100	255	100	309	100	283	100

[a] Percent of base peak.

Table 4
Positive APCI of **2a**–**2g**

	2a		**2b**		**2c**		**2d**		**2e**		**2f**		**2g**	
	18:3	%[a]	18:2	%	16:1	%	18:1	%	16:0	%	20:1	%	18:0	%
$[M+H]^+$	765	100	767	100	741	100	769	100	743	100	797	100	771	100
$[M+H-RCO]^+$	504	20	504	12	504	14	504	9	504	12	504	10	504	11
$[M+H-Glc-RCO]^+$	342	27	342	24	342	22	342	21	342	23	342	19	342	21
$[M+H-Glc-RCO-C_4H_8]^+$	286	14	286	17	286	16	286	18	286	12	286	19	286	17

[a] Percent of base peak.

tion. As a result, 500 °C was set as the operating temperature in both APCI modes.

The negative ion APCI spectra of all the acylated glycosides show intense deprotonated molecules and some intense fragment ions. The relative abundances of the adduct ions increased with increasing formic acid concentration and polarity of the analyte. In negative ion APCI, the eluent composition has no significant effect on the ionization efficiency of acylated glycosides.

The highest responses recorded by using TIC were obtained with an acidic mixture (water–CH_3CN–CH_2Cl_2) as eluent, although the responses recorded by selected ion chromatograms do not show any significant differences caused by different eluent pH. Based on the chromatographic behavior of the acylated glycosides, the mobile phase with formic acid (pH 4.0) was found to be the most suitable in negative ion APCI.

Chromatography of both fractions by an LC–APCI-MS system with detection in the positive and negative ion mode identified compounds **1a**–**1g** and **2a**–**2g**, respectively. LC–MS analysis at m/z 200–1200 of the extract using an APCI showed $[M+H]^+$ (pseudomolecular ions) for the peaks characteristic for acylated xanthosides and allowed the attribution

Table 5
Negative APCI of **2a**–**2g**

	2a		**2b**		**2c**		**2d**		**2e**		**2f**		**2g**	
	18:3	%[a]	18:2	%	16:1	%	18:1	%	16:0	%	20:1	%	18:0	%
$[M-H]^-$	763	84	765	81	739	73	767	62	741	67	795	56	769	53
$[M-H-R_1C=C=O]^-$	503	19	503	12	503	17	503	18	503	13	503	9	503	12
$[M-H-RCOOH]^-$	485	48	485	51	485	37	485	42	485	45	485	49	485	46
$[M-H-RCOOH-Glc]^-$	323	9	323	8	323	9	323	7	323	7	323	6	323	9
$[RCOO]^-$	277	100	279	100	253	100	281	100	255	100	309	100	283	100

[a] Percent of base peak.

of their molecular masses. The $[M+H]^+$ peaks of both A and B series were obtained. For the first series (acylated umbilicaxanthosides B) we obtained the following values of pseudomolecular ions (m/z 971, 973, 995, 997, 999, 1001 and 1027). The second series (acylated umbilicaxanthosides A) contained $[M+H]^+$ at m/z 741, 743, 765, 767, 769, 771 and 797). This analysis allowed us to identify a total of 14 acylated xanthosides in both fractions (i.e., compounds **1a**–**1g** in fraction 1 and **2a**–**2g** in fraction 2).

With the fragmenter voltage set at 40 V, all compounds with positive APCI exhibited a strong $[M+H]^+$ peak, but no fragmentation was observed (data not shown). Some fragmentation of the **1a** (linolenoyl umbilicaxanthoside B) molecule was evident with a fragmenter voltage of 140 V (Fig. 3 and Table 2). The parent ion at m/z 995 $[M+H]^+$ dissociates to six ions (m/z 833 $[M+H–Glc]^+$, m/z 734 $[M+H–RCO]^+$, m/z 572 $[M+H–Glc–RCO]^+$, m/z 410 $[M+H–2\times Glc–RCO]^+$, m/z 354 $[M+H–2\times Glc–RCO–C_4H_8]^+$ and m/z 298 $[M+H–2\times Glc–RCO–2\times C_4H_8]^+$). Fig. 4 shows a tentative pathway for the mass spectral fragmentation of umbilicaxanthoside **1a**. The other 13 compounds had very similar mass spectra, viz. Tables 2–5.

A similar fragmentation was observed in the negative mode (negative APCI). The pseudomolecular ion (compound **1a**, see Fig. 5) at m/z 993 $[M–H]^-$ dissociates to five ions m/z 831 $[M–H–Glc]^-$, m/z 733 $[M–H–R_1C{=}C{=}O]^-$, m/z 715 $[M–H–RCOOH]^-$, m/z 391 $[M–H–2\times Glc–RCOOH]^-$ and m/z 277 $[RCOO]^-$. Again, the remaining compounds (**1b**–**1g** and **2a**–**2g**) give similar mass spectra.

The number of papers which described the positive soft ionization of xanthones is very low. Two papers [3,4] describe the splitting of a pseudomolecular ion most frequently ($[M+Na]^+$), only aglycone being produced ($[A+H]^+$). The study by da Costa et al. [2] describes further splitting of xanthone cycles but the full description of the splitting structures is unfortunately missing. The splitting of two prenyl chains is the only feature which the same in our compounds and those described in the literature.

The identification of the major compounds was done by manual collection of material from major

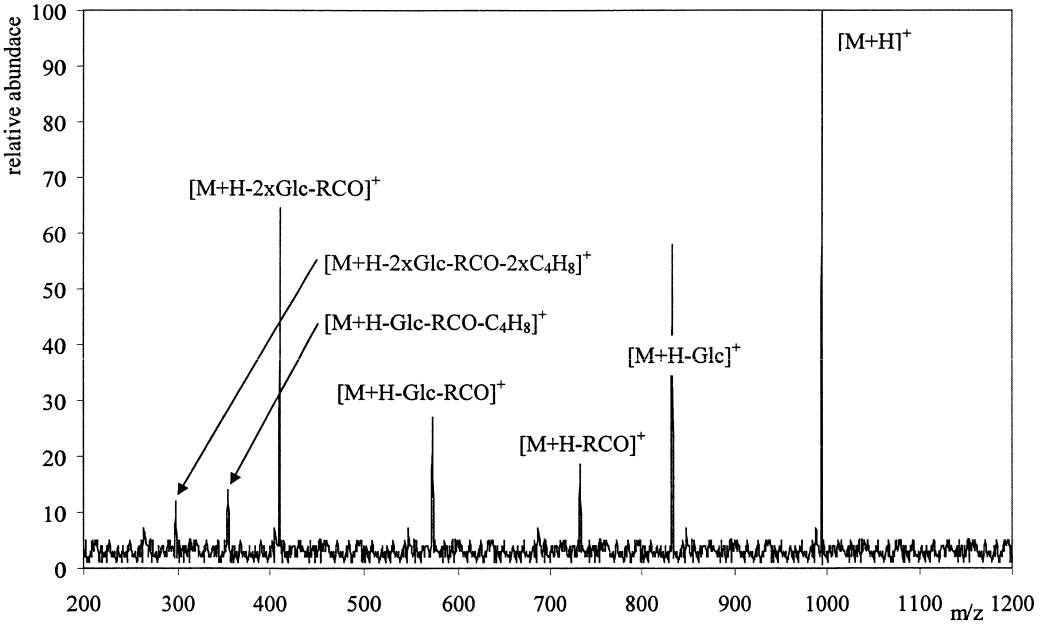

Fig. 3. Some fragmentation of the **1a** (linolenoyl umbilicaxanthoside B) in positive ion mode LC–APCI-MS at fragmenter voltage 140 V.

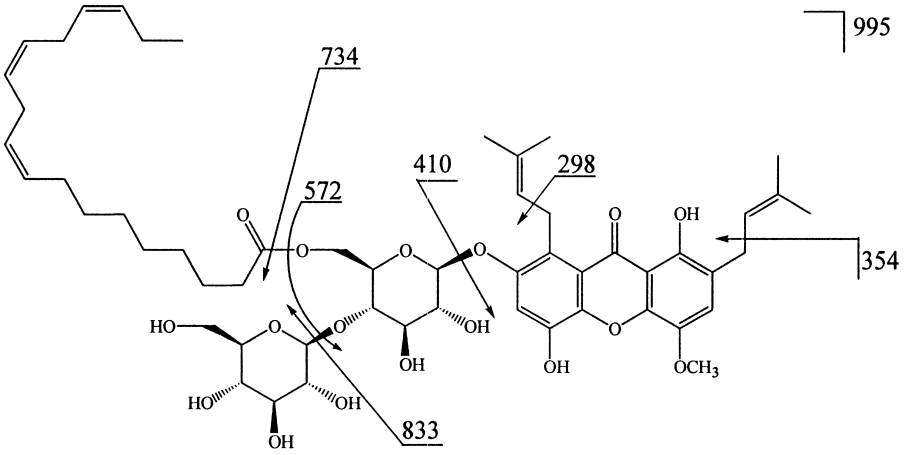

Fig. 4. A tentative pathway for the mass spectral fragmentation of linolenoyl umbilicaxanthoside B (**1a**).

LC peaks, followed by NMR analysis (Table 6). After subtraction of the anomeric signals of the sugars linked at the C_7 position from the total spectrum, the signals of two sugars linked to the aglycone by a glycosidic linkage remained. The correlation in the HMQC (Heteronuclear Multiple Quantum Coherence) spectrum situated apart from other δ_C/δ_H 99.8/5.05 (1H, *d*, $J=8.1$ Hz) showed that the glucose residue was attached to the phenolic function of the aglycone by an ether linkage. This conclusion was confirmed by the HMBC (Heteronuclear Multiple Bond Correlation) experiments, which showed a correlation between the glucose I ($\delta_{H'''}$ 5.05) and C-7 (δ 153.2) of the aglycone, confirming

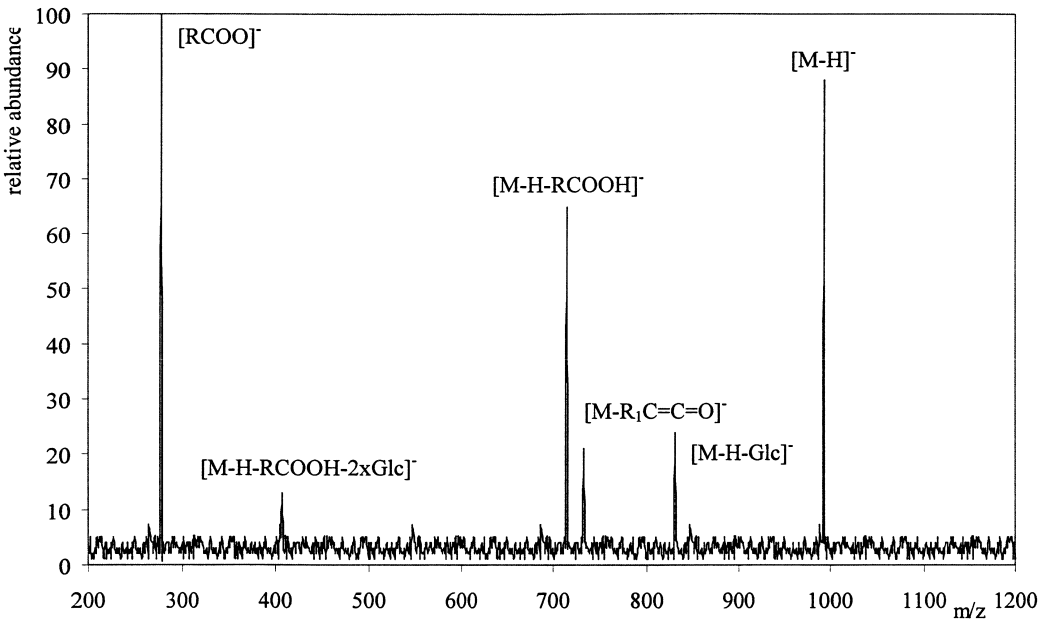

Fig. 5. Some fragmentation of the **1a** (linolenoyl umbilicaxanthoside B) in negative ion mode LC–APCI-MS at fragmenter voltage 140 V.

Table 6
^{1}H and ^{13}C NMR data for linolenoyl umbilicaxanthoside B (**1a**)

Position	^{13}C	$^{1}H(J)$	Position	^{13}C	$^{1}H(J)$
1	151.0	–	4‴	76.7	3.05 (1H, *dd*, *J*=9.3, 8.9)
2	117.8	–	5‴	76.1	3.54 (1H, *m*)
3	119.4	6.47 (1H, *s*)	6‴	65.3	4.03 (1H, *dd*, *J*=12.1, 5.2)
					4.51 (1H, *dd*, *J*=12.1, 2.3)
4	143.2	–	1⁗	104.1	5.15 (1H, *d*, *J*=8.0)
4a	141.3	–	2⁗	73.8	3.52 (1H, *dd*, *J*=9.0, 8.0)
5a	135.7	–	3⁗	76.5	3.61 (1H, *t*, *J*=9.0)
5	147.1	–	4⁗	69.7	3.41 (1H, *t*, *J*=9.0)
6	103.7	6.42 (1H, *s*)	5⁗	76.9	3.45 (1H, *m*)
7	153.2	–	6⁗	62.6	3.72 (1H, *dd*, *J*=12.1, 5.2)
					3.93 (1H, *dd*, *J*=12.1, 2.2)
8	118.4	–	1⁗⁗	172.0	–
8a	129.6	–	2⁗⁗	34.6	2.25 (2H, *m*)
9	183.1	–	3⁗⁗	25.0	1.68 (2H, *m*)
9a	114.6	–	4⁗⁗	29.2	1.29 (6H, *m*)
1-OH	–	13.30*s*	5⁗⁗	29.3	1.29 (6H, *m*)
3-OCH_3	56.3	3.75 (3H, *s*)	6⁗⁗	29.1	1.29 (6H, *m*)
1′	25.4	3.38 (2H, *d*, *J*=7.2)	7⁗⁗	30.3	1.33 (2H, *m*)
2′	123.8	5.39 (1H, *dd*, *J*=7.2, 1.2)	8⁗⁗	27.3	1.96 (2H, *m*)
3′	130.9	–	9⁗⁗	131.8	5.37 (1H, *m*)
4′	26.2	1.65 (3H, *s*)	10⁗⁗	131.7	5.42 (1H, *m*)
5′	18.4	1.79 (3H, *s*)	11⁗⁗	25.7	2.68 (2H, *m*)
1″	26.1	4.19 (2H, *d*, *J*=6.8)	12⁗⁗	128.3	5.35 (1H, *m*)
2″	124.8	5.37 (1H, *dd*, *J*=6.8, 1.5)	13⁗⁗	128.4	5.35 (1H, *m*)
3″	132.0		14⁗⁗	25.6	2.73 (2H, *m*)
4″	25.9	1.67 (3H, *s*)	15⁗⁗	127.1	5.43 (1H, *m*)
5″	18.0	1.84 (3H, *s*)	16⁗⁗	131.9	5.36 (1H, *m*)
1‴	99.8	5.05 (1H, *d*, *J*=8.1)	17⁗⁗	20.6	1.93 (2H, *m*)
2‴	74.2	3.50 (1H, *dd*, *J*=8.9, 8.1)	18⁗⁗	14.2	1.06 (3H, *t*, *J*=6.8)
3‴	77.1	3.58 (1H, *t*, *J*=8.9)			

the attachment of glucose at C-7. Another correlation in the HMQC spectrum between the carbon at δ 65.3 and the deshielded H-6‴ at δ 4.03 and 4.51, respectively, corresponds to the geminal proton of one primary alcoholic function esterified by a long chain fatty acid. From the cross peak in the COSY spectrum of **1a** it was also easy to recognize the anomeric proton of glucose ($\delta_{H\text{-}1'''}$ 5.05) and the H-2‴, H-3‴, H-4‴, H-5‴ and deshielded H-6‴ (δ 4.03 and 4.51). Furthermore, the HMBC experiment showed long range couplings between the deshielded H-6‴ and C-2‴, C-3‴, C-5‴, between the H-6‴ and C-5‴, C_4''', confirming that C-6‴ was esterified by a long chain fatty acid. Other correlations between H-1⁗ and C-2‴ indicated that glucose I was linked to glucose II by a 1–4 linkage. The attachment point of fatty acyl to C-6‴ of glucose was confirmed by comparison of the ^{13}C NMR spectral data of **1a** and xanthoside B obtained after mild alkaline hydrolysis of **1a**. All signals due to the aglycone and sugar moieties appeared at almost the same positions. With regard to the glucose carbon region, on going from **1a** to **1** [7] the signal for C-6 was displayed downfield by +2.7 ppm while both signals due to C-5 and C_4 were shielded by −2.6 and −1.5 ppm, respectively. Such change in the chemical shifts can only be explained if the hydroxyl group at the C-6‴ position of the glucose moiety is acylated.

The presented interpretation of these spectra is the

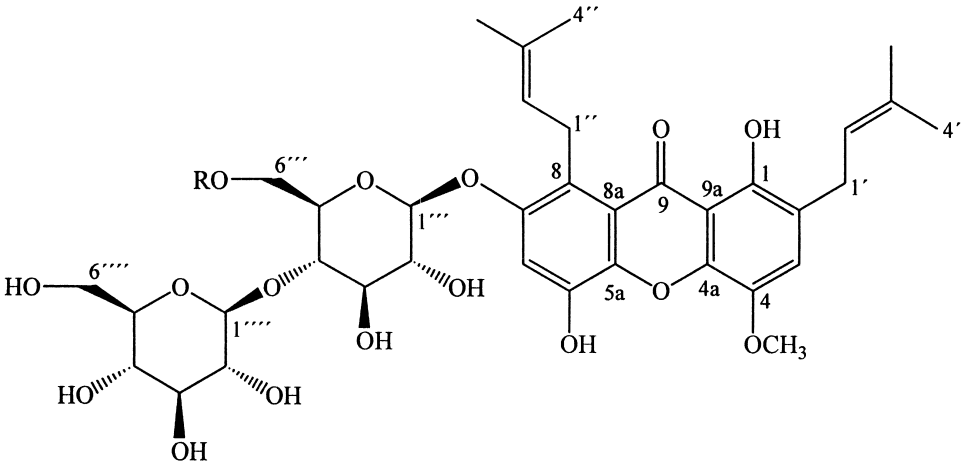

1a R = linolenoyl (1′′′′′ = COO; 18′′′′′ = CH_3)
1b R = linoleoyl
1c R = palmitoleoyl
1d R = oleoyl
1e R = palmitoyl
1f R = eicosenoyl
1g R = stearoyl

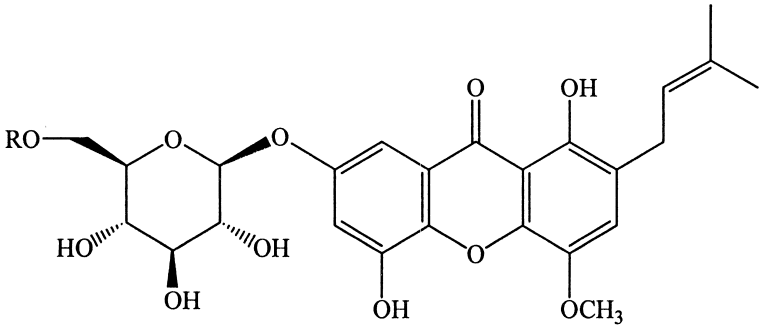

2a R = linolenoyl
2b R = linoleoyl
2c R = palmitoleoyl
2d R = oleoyl
2e R = palmitoyl
2f R = eicosenoyl
2g R = stearoyl

Fig. 6. The structures of all 14 compounds (acylated umbilicaxanthosides B and A) isolated from the lichen *Umbilicaria proboscidea*.

most consistent with the observed data and has been based on the literature describing comprehensive MS analyses of the same or similar compounds [3–6].

4. Conclusion

Fourteen acylated xanthosides (Fig. 6) were studied with APCI–MS in both positive- and negative-ion modes. In general, the negative-ion mode yielded more intense ion signals than did the positive-ion mode. Therefore, the negative-ion mode may be more suitable for quantitative LC–MS analysis of acylated xanthosides. However, because more structural information on acylated xanthosides can be obtained from product ion mass spectra in the positive-ion mode, this mode is useful for the characterization of acylated xanthosides, especially of unknown ones.

The ion signal intensities of $[M+H]^+$ in the positive-ion mode and $[M–H]^-$ in the negative-ion mode generated under optimal APCI conditions are illustrated in Tables 2–5. In general, the signal intensities of $[M–H]^-$ ions of all acylated xanthosides were higher than those of $[M+H]^+$ ions.

Sampling cone voltage is a critical parameter that affects the intensity and distribution of acylated xanthoside ions in both positive- and negative-ion modes so much that markedly different mass spectra can be observed upon variation of the sampling cone voltage.

References

[1] K. Robards, M. Antolovich, Analyst 122 (1997) R11.
[2] C.T. da Costa, J.J. Dalluge, M.J. Welch, B. Coxon, S.A. Margolis, D. Horton, J. Mass Spectrom. 35 (2000) 540.
[3] J.L. Wolfender, S. Rodriguez, K. Hostettmann, J. Chromatogr. A 794 (1998) 299.
[4] S. Rodriguez, J.L. Wolfender, G. Odontuya, O. Purev, K. Hostettmann, Phytochemistry 40 (1995) 1265.
[5] C. Terreaux, M. Maillard, M.P. Gupta, K. Hostettmann, Phytochemistry 40 (1995) 1791.
[6] Z. Szucs, B. Danos, S. Nyiredy, Chromatographia 56 (2002) S19.
[7] T. Rezanka, J. Jachymova, V.M. Dembitsky, Phytochemistry 62 (2003) 607.
[8] H.H. Perkampus, I. Sandemann, C.J. Timmons, DMS UV Atlas organischer Verbindungen, Vols. 1–5, Verlag Chemie, Weinheim, 1966–1971.
[9] E.G. Blight, W.J. Dyer, Can. J. Biochem. Physiol. 37 (1959) 911.
[10] R.C. Murphy, Mass spectrometry of lipids, in: Handbook of Lipid Research, Plenum, New York, 1993.